

5-26-2019

Diagnostic value of two dimensional shear wave elastography combined with texture analysis in early liver fibrosis.

Zhao-Cheng Jian

Capital Medical University; Affiliated Hospital of Weifang Medical University

Jin-Feng Long

Affiliated Hospital of Weifang Medical University

Yu-Jiang Liu

Capital Medical University

Xiang-Dong Hu

Capital Medical University

Ji-Bin Liu

Thomas Jefferson University

Follow this and additional works at: <https://jdc.jefferson.edu/radiologyfp>

 [Part of the Faculty Publications Commons](#)

[Let us know how access to this document benefits you](#)

Recommended Citation

Jian, Zhao-Cheng; Long, Jin-Feng; Liu, Yu-Jiang; Hu, Xiang-Dong; Liu, Ji-Bin; Shi, Xian-Quan; Li, Wei-Sheng; and Qian, Lin-Xue, "Diagnostic value of two dimensional shear wave elastography combined with texture analysis in early liver fibrosis." (2019). *Department of Radiology Faculty Papers*. Paper 63.

<https://jdc.jefferson.edu/radiologyfp/63>

This Article is brought to you for free and open access by the Jefferson Digital Commons. The Jefferson Digital Commons is a service of Thomas Jefferson University's [Center for Teaching and Learning \(CTL\)](#). The Commons is a showcase for Jefferson books and journals, peer-reviewed scholarly publications, unique historical collections from the University archives, and teaching tools. The Jefferson Digital Commons allows researchers and interested readers anywhere in the world to learn about and keep up to date with Jefferson scholarship. This article has been accepted for inclusion in Department of Radiology Faculty Papers by an authorized administrator of the Jefferson Digital Commons. For more information, please contact: JeffersonDigitalCommons@jefferson.edu.

Authors

Zhao-Cheng Jian, Jin-Feng Long, Yu-Jiang Liu, Xiang-Dong Hu, Ji-Bin Liu, Xian-Quan Shi, Wei-Sheng Li, and Lin-Xue Qian

World Journal of *Clinical Cases*

World J Clin Cases 2019 May 26; 7(10): 1093-1241



ORIGINAL ARTICLE**Retrospective Cohort Study**

- 1093 Impact of perioperative transfusion in patients undergoing resection of colorectal cancer liver metastases: A population-based study
Long B, Xiao ZN, Shang LH, Pan BY, Chai J

Retrospective Study

- 1103 Analysis of 24 patients with Achenbach's syndrome
Ada F, Kasimzade F
- 1111 Risk factors and clinical responses of pneumonia patients with colistin-resistant *Acinetobacter baumannii-calcoaceticus*
Aydemir H, Tuz HI, Piskin N, Celebi G, Kulah C, Kokturk F

Observational Study

- 1122 Diagnostic value of two dimensional shear wave elastography combined with texture analysis in early liver fibrosis
Jian ZC, Long JF, Liu YJ, Hu XD, Liu JB, Shi XQ, Li WS, Qian LX

CASE REPORT

- 1133 Selective dorsal rhizotomy in cerebral palsy spasticity - a newly established operative technique in Slovenia: A case report and review of literature
Velnar T, Spazzapan P, Rodi Z, Kos N, Bosnjak R
- 1142 Invasive myxopapillary ependymoma of the lumbar spine: A case report
Strojnik T, Bujas T, Velnar T
- 1149 Electrohydraulic lithotripsy and rendezvous nasal endoscopic cholangiography for common bile duct stone: A case report
Kimura K, Kudo K, Yoshizumi T, Kurihara T, Yoshiya S, Mano Y, Takeishi K, Itoh S, Harada N, Ikegami T, Ikeda T
- 1155 F-18 fluorodeoxyglucose positron emission tomography/computed tomography image of gastric mucormycosis mimicking advanced gastric cancer: A case report
Song BI
- 1161 Ultrasound guidance for transforaminal percutaneous endoscopic lumbar discectomy may prevent radiation exposure: A case report
Zhang MB, Yan LT, Li SP, Li YY, Huang P

- 1169** Retroperitoneoscopic approach for partial nephrectomy in children with duplex kidney: A case report
Chen DX, Wang ZH, Wang SJ, Zhu YY, Li N, Wang XQ
- 1177** Small cell lung cancer with panhypopituitarism due to ectopic adrenocorticotrophic hormone syndrome: A case report
Jin T, Wu F, Sun SY, Zheng FP, Zhou JQ, Zhu YP, Wang Z
- 1184** Therapeutic plasma exchange and a double plasma molecular absorption system in the treatment of thyroid storm with severe liver injury: A case report
Tan YW, Sun L, Zhang K, Zhu L
- 1191** Multiple rare causes of post-traumatic elbow stiffness in an adolescent patient: A case report and review of literature
Pan BQ, Huang J, Ni JD, Yan MM, Xia Q
- 1200** Liquorice-induced severe hypokalemic rhabdomyolysis with Gitelman syndrome and diabetes: A case report
Yang LY, Yin JH, Yang J, Ren Y, Xiang CY, Wang CY
- 1206** Hepatitis B virus-related liver cirrhosis complicated with dermatomyositis: A case report
Zhang J, Wen XY, Gao RP
- 1213** Small cell lung cancer starting with diabetes mellitus: Two case reports and literature review
Zhou T, Wang Y, Zhao X, Liu Y, Wang YX, Gang XK, Wang GX
- 1221** Significant benefits of osimertinib in treating acquired resistance to first-generation EGFR-TKIs in lung squamous cell cancer: A case report
Zhang Y, Chen HM, Liu YM, Peng F, Yu M, Wang WY, Xu H, Wang YS, Lu Y
- 1230** Successful endoscopic extraction of a proximal esophageal foreign body following accurate localization using endoscopic ultrasound: A case report
Wang XM, Yu S, Chen X
- 1234** Minimally invasive endoscopic maxillary sinus lifting and immediate implant placement: A case report
Mudalal M, Sun XL, Li X, Fang J, Qi ML, Wang J, Du LY, Zhou YM

ABOUT COVER

Editorial Board Member of *World Journal of Clinical Cases*, Abdullah Ozkok, MD, Associate Professor, Department of Internal Medicine and Nephrology, University of Health Sciences, Umraniye Training and Research Hospital, Istanbul, Turkey

AIMS AND SCOPE

World Journal of Clinical Cases (*World J Clin Cases*, *WJCC*, online ISSN 2307-8960, DOI: 10.12998) is a peer-reviewed open access academic journal that aims to guide clinical practice and improve diagnostic and therapeutic skills of clinicians.

The primary task of *WJCC* is to rapidly publish high-quality Case Report, Clinical Management, Editorial, Field of Vision, Frontier, Medical Ethics, Original Articles, Meta-Analysis, Minireviews, and Review, in the fields of allergy, anesthesiology, cardiac medicine, clinical genetics, clinical neurology, critical care, dentistry, dermatology, emergency medicine, endocrinology, family medicine, gastroenterology and hepatology, etc.

INDEXING/ABSTRACTING

The *WJCC* is now indexed in PubMed, PubMed Central, Science Citation Index Expanded (also known as SciSearch®), and Journal Citation Reports/Science Edition. The 2018 Edition of Journal Citation Reports cites the 2017 impact factor for *WJCC* as 1.931 (5-year impact factor: N/A), ranking *WJCC* as 60 among 154 journals in Medicine, General and Internal (quartile in category Q2).

RESPONSIBLE EDITORS FOR THIS ISSUE

Responsible Electronic Editor: *Yun-Xiaojuan Wu* Proofing Editorial Office Director: *Jin-Lei Wang*

NAME OF JOURNAL

World Journal of Clinical Cases

ISSN

ISSN 2307-8960 (online)

LAUNCH DATE

April 16, 2013

FREQUENCY

Semimonthly

EDITORS-IN-CHIEF

Dennis A Bloomfield, Sandro Vento

EDITORIAL BOARD MEMBERS

<https://www.wjgnet.com/2307-8960/editorialboard.htm>

EDITORIAL OFFICE

Jin-Lei Wang, Director

PUBLICATION DATE

May 26, 2019

COPYRIGHT

© 2019 Baishideng Publishing Group Inc

INSTRUCTIONS TO AUTHORS

<https://www.wjgnet.com/bpg/gerinfo/204>

GUIDELINES FOR ETHICS DOCUMENTS

<https://www.wjgnet.com/bpg/GerInfo/287>

GUIDELINES FOR NON-NATIVE SPEAKERS OF ENGLISH

<https://www.wjgnet.com/bpg/gerinfo/240>

PUBLICATION MISCONDUCT

<https://www.wjgnet.com/bpg/gerinfo/208>

ARTICLE PROCESSING CHARGE

<https://www.wjgnet.com/bpg/gerinfo/242>

STEPS FOR SUBMITTING MANUSCRIPTS

<https://www.wjgnet.com/bpg/GerInfo/239>

ONLINE SUBMISSION

<https://www.f6publishing.com>

Observational Study

Diagnostic value of two dimensional shear wave elastography combined with texture analysis in early liver fibrosis

Zhao-Cheng Jian, Jin-Feng Long, Yu-Jiang Liu, Xiang-Dong Hu, Ji-Bin Liu, Xian-Quan Shi, Wei-Sheng Li, Lin-Xue Qian

ORCID number: Zhao-Cheng Jian (0000-0003-0159-507X); Jin-Feng Long (0000-0001-7929-8433); Yu-Jiang Liu (0000-0002-4007-4413); Xiang-Dong Hu (0000-0001-5496-6685); Ji-Bin Liu (0000-0003-2979-9162); Xian-Quan Shi (0000-0002-7424-0360); Wei-Sheng Li (0000-0002-0961-1559); Lin-Xue Qian (0000-0001-7116-0608).

Author contributions: All authors helped to perform the research; Jian ZC manuscript writing, performing procedures and data analysis; Long JF contribution to writing the manuscript, performing experiments, and data analysis; Liu YJ and Hu XD contribution to performing experiments; Liu JB contribution to writing the manuscript; Shi XQ and Li WS contribution to data analysis; Qian LX manuscript writing, drafting conception and design, performing experiments, and data analysis.

Institutional review board statement: This study was reviewed and approved by the Ethics Committee of Beijing Friendship Hospital, Capital Medical University.

Informed consent statement: Patient's informed consent was obtained before the study, though the clinical data used in this study were anonymous.

Conflict-of-interest statement: All authors declare no conflicts-of-interest related to this article.

Zhao-Cheng Jian, Yu-Jiang Liu, Xiang-Dong Hu, Xian-Quan Shi, Wei-Sheng Li, Lin-Xue Qian, Department of Ultrasound, Beijing Friendship Hospital, Capital Medical University, Beijing 100050, China

Zhao-Cheng Jian, Jin-Feng Long, Medical Imaging Center, Affiliated Hospital of Weifang Medical University, Weifang 261031, Shandong Province, China

Ji-Bin Liu, Institute of Ultrasound, Thomas Jefferson University Hospital, Philadelphia, PA 19107, United States

Corresponding author: Lin-Xue Qian, MD, Chief Doctor, Department of Ultrasound, Beijing Friendship Hospital, Capital Medical University, No. 95 Yong'an Road, Xicheng District, Beijing 100050, China. qianlinxue2002@163.com

Telephone: +86-13562645007

Fax: +86-10-63138576

Abstract**BACKGROUND**

Staging diagnosis of liver fibrosis is a prerequisite for timely diagnosis and therapy in patients with chronic hepatitis B. In recent years, ultrasound elastography has become an important method for clinical noninvasive assessment of liver fibrosis stage, but its diagnostic value for early liver fibrosis still needs to be further improved. In this study, the texture analysis was carried out on the basis of two dimensional shear wave elastography (2D-SWE), and the feasibility of 2D-SWE plus texture analysis in the diagnosis of early liver fibrosis was discussed.

AIM

To assess the diagnostic value of 2D-SWE combined with textural analysis in liver fibrosis staging.

METHODS

This study recruited 46 patients with chronic hepatitis B. Patients underwent 2D-SWE and texture analysis; Young's modulus values and textural patterns were obtained, respectively. Textural pattern was analyzed with regard to contrast, correlation, angular second moment (ASM), and homogeneity. Pathological results of biopsy specimens were the gold standard; comparison and assessment of the diagnosis efficiency were conducted for 2D-SWE, texture analysis and their combination.

Data sharing statement: No additional data are available.

STROBE statement: The authors have read the STROBE Statement – checklist of items, and the manuscript was prepared and revised according to the STROBE Statement – checklist of items.

Open-Access: This article is an open-access article which was selected by an in-house editor and fully peer-reviewed by external reviewers. It is distributed in accordance with the Creative Commons Attribution Non Commercial (CC BY-NC 4.0) license, which permits others to distribute, remix, adapt, build upon this work non-commercially, and license their derivative works on different terms, provided the original work is properly cited and the use is non-commercial. See: <http://creativecommons.org/licenses/by-nc/4.0/>

Manuscript source: Unsolicited manuscript

Received: February 2, 2019

Peer-review started: February 2, 2019

First decision: March 10, 2019

Revised: March 19, 2019

Accepted: April 8, 2019

Article in press: April 9, 2019

Published online: May 26, 2019

P-Reviewer: Chamberlain MC, Gilbert MR, Jones G

S-Editor: Wang JL

L-Editor: A

E-Editor: Wu YXJ



RESULTS

2D-SWE displayed diagnosis efficiency in early fibrosis, significant fibrosis, severe fibrosis, and early cirrhosis (AUC > 0.7, $P < 0.05$) with respective AUC values of 0.823 (0.678-0.921), 0.808 (0.662-0.911), 0.920 (0.798-0.980), and 0.855 (0.716-0.943). Contrast and homogeneity displayed independent diagnosis efficiency in liver fibrosis stage (AUC > 0.7, $P < 0.05$), whereas correlation and ASM showed limited values. AUC of contrast and homogeneity were respectively 0.906 (0.779-0.973), 0.835 (0.693-0.930), 0.807 (0.660-0.910) and 0.925 (0.805-0.983), 0.789 (0.639-0.897), 0.736 (0.582-0.858), 0.705 (0.549-0.883) and 0.798 (0.650-0.904) in four liver fibrosis stages, which exhibited equivalence to 2D-SWE in diagnostic efficiency ($P > 0.05$). Combined diagnosis (PRE) displayed diagnostic efficiency (AUC > 0.7, $P < 0.01$) for all fibrosis stages with respective AUC of 0.952 (0.841-0.994), 0.896 (0.766-0.967), 0.978 (0.881-0.999), 0.947 (0.835-0.992). The combined diagnosis showed higher diagnosis efficiency over 2D-SWE in early liver fibrosis ($P < 0.05$), whereas no significant differences were observed in other comparisons ($P > 0.05$).

CONCLUSION

Texture analysis was capable of diagnosing liver fibrosis stage, combined diagnosis had obvious advantages in early liver fibrosis, liver fibrosis stage might be related to the hepatic tissue hardness distribution.

Key words: Elastography; Two-dimensional shear wave; Texture analysis; Liver fibrosis; Staging

©The Author(s) 2019. Published by Baishideng Publishing Group Inc. All rights reserved.

Core tip: This study explored the diagnostic value of texture analysis in early liver fibrosis in patients with chronic hepatitis B on the basis of two dimensional shear wave elastography. It demonstrated that texture analysis was capable of diagnosing liver fibrosis, combined diagnosis had obvious advantages in early liver fibrosis, and the liver fibrosis stage might be related to the spatial heterogeneity of hepatic tissue hardness distribution.

Citation: Jian ZC, Long JF, Liu YJ, Hu XD, Liu JB, Shi XQ, Li WS, Qian LX. Diagnostic value of two dimensional shear wave elastography combined with texture analysis in early liver fibrosis. *World J Clin Cases* 2019; 7(10): 1122-1132

URL: <https://www.wjgnet.com/2307-8960/full/v7/i10/1122.htm>

DOI: <https://dx.doi.org/10.12998/wjcc.v7.i10.1122>

INTRODUCTION

Liver fibrosis is an important stage in the development of chronic hepatitis B. Its progression can be halted or even reversed by early diagnosis, dynamic assessment and effective treatment. Identification of the fibrosis stage is thus an essential requisite for timely diagnosis and therapy^[1]. Liver biopsy is considered the gold standard for diagnosis of cirrhosis and staging of fibrosis; however, biopsy is an invasive procedure the clinical application of which is restrained due to poor patient compliance and sampling error^[2,3]. Hence, an accurate and non-invasive method to determine fibrosis stage is urgently required in the clinic. Ultrasound elastography is rapidly advancing and is becoming an important clinical measure for the detection of liver fibrosis stage^[4]. This is demonstrated by the clinical guidelines published by the European Federation of Societies for Ultrasound in Medicine and Biology^[5] and World Federation for Ultrasound in Medicine and Biology^[6]. At present, transient elastography (TE) and two dimensional shear wave elastography (2D-SWE) are hot topics. This is demonstrated by previous studies^[7,8] involving the diagnosis of liver fibrosis which focused on significant liver fibrosis ($\geq F2$), whereas less has been reported regarding the diagnosis of early liver fibrosis (F1). In this study, on the basis of 2D-SWE in patients with chronic hepatitis B, the textural features of the designated elastic image were derived from gray-level co-occurrence matrix (GLCM) built by

texture analysis software. These results were compared with pathological results of liver biopsies and statistical analyses were conducted to explore the feasibility of 2D-SWE plus texture analysis in the diagnosis of early liver fibrosis stage.

MATERIALS AND METHODS

Subjects

This study recruited patients with chronic hepatitis B who were scheduled for percutaneous liver biopsy at Beijing Friendship Hospital, Capital Medical University (Beijing, China) between September 2016 and September 2017 and included 20 males and 26 females with ages ranging from 15-71 years (mean age of 45.1 ± 13.5 years). Exclusion criteria were patients in whom elastography failed or biopsy specimens didn't meet the quality requirements for pathological diagnosis. This study was reviewed and approved by the Ethical Committee of Beijing Friendship Hospital, Capital Medical University. All patients or their guardians signed the informed consent.

Instruments and methods

Instruments and parameter set-up: SuperSonic Imagine Aixplorer ultrasound system (Aixplorer®, SuperSonic Imagine, Aix-en-Provence, France) was used with parameters as follows: SC6-1 convex lens probe and probe frequency of 1-6 MHz; image depth of 8 cm, image enlargement to 120%; elastography sampling frame at 4 cm × 3 cm; region of interest (ROI) of 15 ± 2 mm; elastic measurement scale of 40 kPa; 2D image elastic images arrayed up and down, elastography sampling frame was placed on the image center.

Ultrasonography: Eight hours of fasting was ordered before ultrasonography. Patients were in the supine position with right upper limb lifted to increase the width of the intercostal space. On the right intercostal space, the right lower sections of the anterior or posterior liver lobe was selected and the probe was properly pressed to clearly display the image while avoiding large intrahepatic ducts. The upper edge of the elastography sampling frame was positioned about 1 cm below the liver capsule. Patients were asked to hold breathing for 3-5 s under the condition of calm respiration. The 2D-SWE mode was switched on and images were frozen upon stable elastic images followed by storage of raw images and measurement and documentation of the mean values (kPa) within ROI. The criteria for elastography failure were: the color filling defect in the elastography sampling frame exceeded half area or the minimum value in ROI was zero. Each patient was measured 3 times, and 3 raw images (for subsequent texture analysis) were stored to yield 3 values of the Young's modulus and the mean value was calculated as well. All patients were examined by the same senior clinician who specialized in ultrasound for more than 5 years and was expert at ultrasound elastography. Data collection was performed by the same clinician as well.

Texture analysis: Texture analysis software (SSI_Toll_Tsinghua, Tsinghua, Beijing, China) was used to delineate the filling area (without filling the defect area) on the raw elastic image. The textural features of the designated area were derived *via* constructing a GLCM. In addition, 4 sets of indexes were acquired from 4 different angles (0°, 45°, 135°, and 180°) including contrast, correlation, angular second moment (ASM), and homogeneity. The mean values were calculated. **Figure 1** illustrates the analysis process. Each patient was measured 3 times, and the individual mean values of contrast, correlation, ASM, and homogeneity were calculated.

Percutaneous liver biopsy: Ultrasound-guided liver biopsy was performed in all patients. The elastography sampling frame region was the biopsy target, and liver tissue of 1.5-2.5 cm length was collected using a 16G biopsy needle (MG1522, Bard, Murray Hill, New Jersey, USA). Under a microscope, more than 10 complete portal areas were collected, and specimens with fractured liver tissue were excluded. Needle biopsies were made 2-3 times for each patient, and collected tissues were fixed in formaldehyde solution prior to sectioning, HE staining, reticular fiber and Masson staining. Diagnosis was made jointly by 2 senior pathologists who reviewed the slides blinded. Liver fibrosis was staged to F0-F4 according to the METAVIR scoring system: F0 referred to no fibrosis; F1 referred to star-shaped enlargement of the portal area but without a fibrous septum; F2 referred to star-shaped enlargement of the portal area with a few fibrous septa; F3 referred to the presence of abundant fibrous septa but without pseudo-lobule formation; F4 referred to numerous fibrous septa with pseudo-lobule formation.

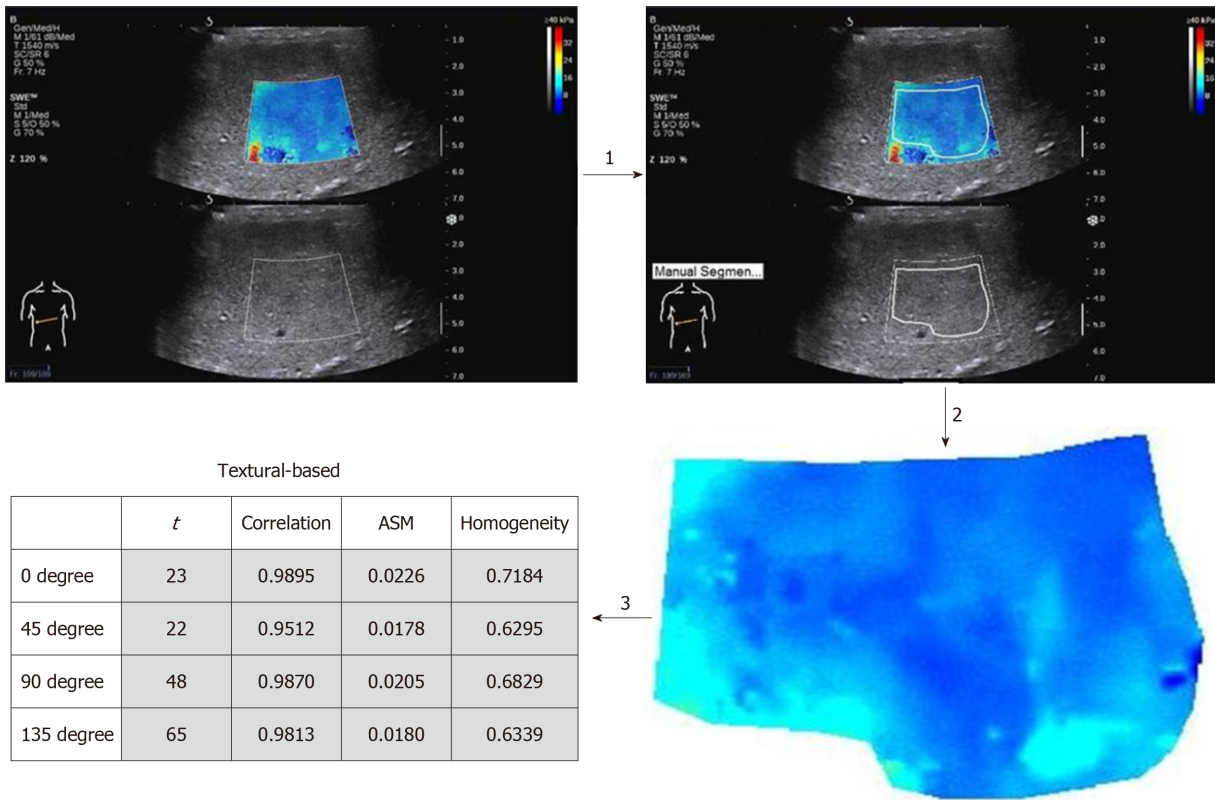


Figure 1 Texture analysis process. Step 1, texture analysis software was used to delineate the filling area (without filling defect area) on the raw elastic image, avoiding vascular and biliary cavities. Step 2, a texture analysis image was generated. Step 3, 4 sets of indexes were acquired from 4 different angles (0°, 45°, 135°, and 180°), including contrast, correlation, angular second moment, and homogeneity. ASM: Angular second moment.

Grouping and inter-group comparisons: Based on the pathological results of liver biopsies, all eligible patients were allocated into different groups of liver fibrosis stages: early liver fibrosis group ($\geq F1$), significant fibrosis group ($\geq F2$), severe fibrosis group ($\geq F3$), and early cirrhosis group (F4). Inter-group comparisons were made accordingly as: F0 vs F1-4; F0-1 vs F2-4; F0-2 vs F3-4; F0-3 vs F4. Totally, statistical analyses were conducted for 4 groups to test the diagnosis efficiency of the aforementioned results in liver fibrosis stage.

Statistical analysis

Statistical analysis was conducted with SPSS 20.0 software (Version 20.0, SPSS Inc., Chicago, IL, USA) and MedCalc statistical software (Version 18.6, MedCalc software, Ostend, Belgium). Data were expressed by median and range, and a Mann-Whitney U test was adopted for making comparison between two independent groups, while Spearman's rank correlation coefficient was used to evaluate the correlation of individual variables with pathological stages. Predictive value (PRE) of combined diagnosis was calculated based on a logistic regression model. In addition, receiver operating characteristic (ROC) curves were plotted, followed by calculation of the area under the ROC curves (AUC) with 95%CI. Diagnostic efficacy was considered when AUC was greater than 0.7. Intra-group AUC comparisons for different variables were analyzed by Hanley and McNeil's method. The threshold value for diagnosis was determined by the highest critical point of Youden's index (YI). Intra-class correlation coefficients (ICC) were adopted to assess consistency in diagnosis, with ICC > 0.75 defined as a good consistency. $P < 0.05$ was considered statistically significant.

RESULTS

Pathological diagnosis

As shown in Table 1, among 46 patients, 44 cases were ultimately enrolled into this study. Two cases were excluded: one case due to failure of 2D-SWE (patient had poor compliance with breathing instruction which rendered filling the ROI less than 50%); the other case was due to fracture of liver biopsy tissue - patient rejected repeated

biopsy.

In 44 cases with complete data, pathological stages encompassed: F0 in 15 cases, F1 in 9 cases, F2 in 9 cases, F3 in 5 cases, and F4 in 6 cases.

Correlation of individual detection results with pathological stage and inter-group comparisons

Rank correlation: Rank correlation analysis displayed: pathological fibrosis stage was statistically correlated with the values of Young's modulus, contrast and homogeneity (r value of 0.659, 0.710 and -0.498, respectively, $P < 0.01$ for all indexes); no significant correlation was detected between pathological fibrosis stage and correlation or ASM (r values of -0.210 and -0.323, respectively).

Inter-group comparison for individual variables: As shown in Table 2, statistical differences were found in all inter-group comparisons for the values of Young's modulus, contrast and homogeneity ($P < 0.05$).

Comparing diagnosis efficiency of liver fibrosis stage

As shown in Figure 2, ROC curves for each group were constructed for 2D-SWE, contrast, correlation, ASM, homogeneity, and PRE of combined diagnosis, respectively. The diagnosis efficiency of each index was analyzed as well.

Diagnosis efficiency of 2D-SWE: 2D-SWE displayed diagnosis efficiency in early liver fibrosis ($\geq F1$), significant liver fibrosis ($\geq F2$), severe liver fibrosis ($\geq F3$), and early cirrhosis (F4) (AUC > 0.7 , $P < 0.05$), with respective AUC of 0.823 (0.678-0.921), 0.808 (0.662-0.911), 0.920 (0.798-0.980) and 0.855 (0.716-0.943), and with cutoff values of 5.967, 8.667, 11.033 and 13.000 kPa. Table 3 shows sensitivity and specificity results.

Diagnosis efficiency of texture analysis: Contrast and homogeneity illustrated diagnosis efficiency in all stages of liver fibrosis (AUC > 0.7 , $P < 0.05$). AUC of contrast in early liver fibrosis ($\geq F1$), significant liver fibrosis ($\geq F2$), severe fibrosis ($\geq F3$), and early cirrhosis (F4) groups were 0.906 (0.779-0.973), 0.835 (0.693-0.930), 0.807 (0.660-0.910), 0.925 (0.805-0.983); AUC of homogeneity in all stages of liver fibrosis were 0.789 (0.639-0.897), 0.736 (0.582-0.858), 0.705 (0.549-0.883), 0.798 (0.650-0.904) respectively. No significant differences were observed in all comparisons with 2D-SWE ($P > 0.05$). Table 3 presents cut-off values, sensitivity, and specificity.

Correlation and ASM showed poor diagnosis efficiency with the exception of ASM, which had diagnostic ability in the early cirrhosis group (AUC > 0.7 , $P < 0.05$).

Diagnosis efficiency for combined diagnosis: PRE of combined diagnosis displayed efficiency in all stages of liver fibrosis (AUC > 0.7 , $P < 0.01$). AUC in early liver fibrosis ($\geq F1$), significant liver fibrosis ($\geq F2$), severe fibrosis ($\geq F3$), and early stage of cirrhosis (F4) groups were 0.952 (0.841-0.994), 0.896 (0.766-0.967), 0.978 (0.881-0.999) and 0.947 (0.835-0.992), respectively. The combined diagnosis showed higher diagnosis efficiency over 2D-SWE in early liver fibrosis ($P < 0.05$), whereas no significant differences were observed in other comparisons ($P > 0.05$). The cut-off values, sensitivity, and specificity are listed in Table 3.

Assessment of consistency in individual detection results

Raw images of two measurements were randomly selected out of the F0 group, followed by consistency assessment in 2D-SWE and textural variables (contrast, correlation, ASM, homogeneity). ICC values were 0.88, 0.98, 0.97, 0.99 and 0.99 (more than 0.75), respectively, indicating a good consistency in various detection results.

DISCUSSION

In recent years, the non-invasive detection technology of liver fibrosis has developed rapidly, especially the ultrasound elastography technology. Significant liver fibrosis and early liver cirrhosis were the focus of previous studies^[9,10], which are considered as important markers of disease progression and initiation of treatment. However, hepatitis B virus DNA and alanine aminotransferase level are the main basis for the initiation of antiviral therapy of chronic hepatitis B patients^[11,12]. The diagnosis of liver fibrosis stage is more important as a means of disease monitoring and therapeutic effect evaluation, so the diagnosis of early liver fibrosis particularly important. Hepatic fibrosis is a dynamic process in which early liver fibrosis indicates the transition from quantitative to qualitative changes of the disease, and indicates that patients require more active monitoring and treatment. In view of this, the ultrasound elastography was combined with the application of texture analysis in this study in order to make progress in the diagnosis of early liver fibrosis.

Table 1 Distribution of patients with liver fibrosis

| Pathological stage | Gender | | Mean age (yr) |
|--------------------|--------|--------|---------------|
| | Male | Female | |
| F0 | 7 | 8 | 36.8 ± 11.1 |
| F1 | 6 | 3 | 39.8 ± 14.9 |
| F2 | 3 | 6 | 52.4 ± 8.6 |
| F3 | 2 | 3 | 49.4 ± 8.1 |
| F4 | 2 | 4 | 59.3 ± 9.3 |

Ultrasound-based elastography technology as currently used widely in clinical applications are mainly TE and 2D-SWE. In clinical practice, TE is adopted universally^[13], which manifests satisfactory diagnostic value to liver fibrosis stage^[14,15]. Nonetheless, because TE is unable to display 2D sonography in real-time, the intrahepatic duct system could interfere with detection, and the measurement accuracy could be affected by the ribs, gas, ascites, and thick subcutaneous fat^[16]. A previous study reported that failure of TE detection resulted in unreliable measurements that accounted for 16.3%^[17]. 2D-SWE can detect the transmission speed of shear waves and generate images *via* super speed image processing technology that produces color elastic images of target tissue. The severity of liver fibrosis is quantified by Young's modulus. It avoids partial defects of TE and shows appropriate diagnosis efficiency^[18,19] and reproducibility^[9,20]. Our study revealed that the cutoff value of 2D-SWE was 8.667, 11.033, and 13.000 kPa in significant liver fibrosis (\geq F2), severe fibrosis (\geq F3), and early stage of cirrhosis (F4), respectively, while the sensitivity/specificity was accordingly 90.0%/58.3%, 90.9%/90.9%, and 83.3%/86.8%, which presents a stable diagnosis efficiency. Given that no liver function or other factors were taken into account for eligible patients enrolled in this study, our results were slightly divergent from previous studies^[9,18-20]. Even though 2D-SWE can overcome some drawbacks associated with TE, the advantages of high sampling range, universal feasibility, and real-time 2D imaging also impose poor diagnosis efficiency in liver fibrosis. In this study, 2D-SWE illustrated some diagnostic value in liver fibrosis with low YI which was only 0.533, but with high-sensitivity and low specificity. It failed to meet the clinical requirements for diagnosis of early liver fibrosis.

Texture analysis is a process of extracting texture feature parameters by certain image processing techniques to obtain a quantitative or qualitative description of the texture. In previous ultrasound elastography studies, texture analysis has demonstrated advantages in the identification of carotid vulnerable plaques, thyroid and breast nodules^[21,22]. In the 2D-SWE inspection, the elastic image is obtained by gray-scale coding of the information of Young's modulus. This study attempts to characterize the texture by extracting the spatial distribution of grayscale *via* creating a GLCM^[23,24] and thereby reflecting the spatial statistical properties of Young's modulus. Then, combined with the Young's modulus value and the pathological results of liver fibrosis, the application value of texture features in the diagnosis of liver fibrosis was analyzed. Textural features encompass contrast, correlation, ASM, and homogeneity. Contrast refers to measurements of local variations in the image; correlation means the linear correlation of gray levels in the image; ASM reflects the order of gray levels in the image; homogeneity, which is also called inverse torque, represents measurement of proximity between element and the diagonal in GLCM and reflects uniformity of the image^[25]. In our study, contrast was positively correlated with liver fibrosis stage, while homogeneity was negatively correlated with liver fibrosis stage. As the degree of liver fibrosis increased, contrast increased and homogeneity decreased, which is consistent with the intuitive features of the obtained image. In the diagnosis of liver fibrosis in all stages, both features have independent diagnosis efficiency (AUC > 0.7, $P < 0.05$), but there is no statistically difference from 2D-SWE. Whereas, correlation and ASM showed limited diagnosis efficiency. Therefore, we believe that it is feasible to obtain and analyze the textural features quantified based on the GLCM, and to take it as a diagnosis index for liver fibrosis stage; contrast and homogeneity harbor potency as an independent index for diagnosis of liver fibrosis stage. Furthermore, It can be inferred that the liver fibrosis patients with the progress of the disease, the overall hardness of the liver tissue increases, while the imbalance of liver tissue hardness distribution is also increasing, that is, the spatial heterogeneity of the hardness distribution is more obvious, the

Table 2 Comparison of two dimensional shear wave elastography and textural features in different groups (Median, Range)

| Comparison | 2D-SWE | P-value | Contrast | P-value | Correlation | P-value | ASM | P-value | Homogeneity | P value | |
|---------------------|--------|--------------------|----------|---------------------|-------------|------------------|-------|---------------------|-------------|------------------|-------|
| F0 vs F1-4 (≥ F1) | F0 | 5.97 (4.07-11.03) | 0.001 | 1.51 (0.44-6.69) | < 0.001 | 0.97 (0.79-0.99) | 0.72 | 0.056 (0.015-0.87) | 0.087 | 0.76 (0.64-0.97) | 0.002 |
| | F1-4 | 10.63 (6.40-44.87) | | 8.39 (1.39-200.76) | | 0.96 (0.67-0.99) | | 0.043 (0.003-0.33) | | 0.54 (0.33-0.87) | |
| F0-1 vs F2-4 (≥ F2) | F0-1 | 7.78 (4.07-17.43) | < 0.001 | 2.66 (0.44-19.64) | < 0.001 | 0.97 (0.79-0.99) | 0.041 | 0.05 (0.015-0.87) | 0.11 | 0.69 (0.59-0.97) | 0.007 |
| | F2-4 | 11.94 (6.4-44.87) | | 11.78 (1.39-200.76) | | 0.94 (0.66-0.98) | | 0.034 (0.003-0.33) | | 0.61 (0.33-0.87) | |
| F0-2 vs F3-4 (≥ F3) | F0-2 | 9.03 (4.07-17.43) | < 0.001 | 3.39 (0.44-27.43) | 0.002 | 0.96 (0.79-0.99) | 0.23 | 0.049 (0.012-0.87) | 0.11 | 0.68 (0.50-0.97) | 0.044 |
| | F3-4 | 14.97 (9.00-44.87) | | 14.86 (1.39-200.76) | | 0.94 (0.67-0.98) | | 0.030 (0.003-0.33) | | 0.59 (0.33-0.87) | |
| F0-3 vs F4 (F4) | F0-3 | 9.42 (4.07-22.23) | 0.004 | 3.69 (0.44-67.49) | < 0.001 | 0.96 (0.74-0.99) | 0.29 | 0.05 (0.012-0.87) | 0.018 | 0.68 (0.50-0.97) | 0.018 |
| | F4 | 17.30 (9.00-44.87) | | 90.43 (9.34-200.76) | | 0.93 (0.67-0.98) | | 0.019 (0.003-0.094) | | 0.50 (0.33-0.69) | |

2D-SWE: Two dimensional shear wave elastography; ASM: Angular second moment.

stage of liver fibrosis may be heavier.

PRE arose from combinatorial diagnosis and exerted optimal performance in the diagnosis of liver fibrosis stage (AUC > 0.7, *P* < 0.05). Compared with the above independent factors in all groups, ROC curve of PRE was more proximal to the left upper corner, while AUC is the greatest value. Combination of 2D-SWE with textural analysis could more accurately reflect liver tissue hardness when the former reflects the absolute elastic modulus values in the region of interest, while the latter reflects the spatial distribution of the elastic modulus in the selected region. Statistical analysis showed that the combined diagnosis of early liver fibrosis was superior to 2D-SWE (*P* < 0.05).

Our study demonstrated that combination of 2D-SWE with texture analysis could effectively improve diagnosis efficiency peculiarly for early liver fibrosis with chronic hepatitis B. Nonetheless, this study contains some drawbacks: on one hand, the sample size was limited, though the feasible of texture analysis in diagnosis of liver fibrosis was conformed, the diagnosis model of liver fibrosis related texture analysis has not yet been established; on the other hand, hepatitis B virus DNA level, liver function and other factors weren't stratified. In particular, alanine aminotransferase, which is very important in the diagnosis and treatment of liver fibrosis with chronic hepatitis B, is not included in this study and may affect the stability of the result. In future studies, more effort should be directed to increasing sample size and simultaneously to comprehensive analysis of relevant indexes. Doing this should provide a novel and effective clinical measure for the non-invasive examination of liver fibrosis, especially of early liver fibrosis.

Table 3 Receiver operating characteristic curve analysis of various indicators in diagnosing pathological stages of liver fibrosis

| | | 2D SWE | Contrast | Correlation | ASM | Homogeneity | PRE |
|---------------------|-------------|---------------------|---------------------|----------------------|---------------------|---------------------|----------------------------------|
| F0 vs F1-4 (≥ F1) | AUC (95%CI) | 0.823 (0.678-0.921) | 0.906 (0.779-0.973) | 0.533 (0.377-0.685) | 0.659 (0.500-0.795) | 0.789 (0.639-0.897) | 0.952 (0.841-0.994) ¹ |
| | <i>P</i> | < 0.0001 | < 0.0001 | 0.735 | 0.09 | < 0.0001 | < 0.0001 |
| | YI | 0.533 | 0.697 | 0.195 | 0.363 | 0.448 | 0.761 |
| | Cutoff | > 5.967 | > 2.726 | ≤ 0.899 | ≤ 0.0940 | ≤ 0.632 | > 0.591 |
| | TPR (%) | 100.0 | 89.7 | 13.8 | 89.7 | 44.8 | 82.8 |
| | TNR (%) | 53.3 | 80.0 | 66.7 | 46.7 | 100.0 | 93.3 |
| F0-1 vs F2-4 (≥ F2) | AUC (95%CI) | 0.808 (0.662-0.911) | 0.835 (0.693-0.930) | 0.680 (0.523-0.813) | 0.641 (0.482-0.780) | 0.736 (0.582-0.858) | 0.896 (0.766-0.967) |
| | <i>P</i> | < 0.0001 | < 0.0001 | 0.0267 | 0.0936 | 0.0023 | < 0.0001 |
| | YI | 0.483 | 0.567 | 0.358 | 0.258 | 0.508 | 0.767 |
| | Cutoff | > 8.667 | > 7.391 | ≤ 0.973 | ≤ 0.0350 | ≤ 0.617 | > 0.440 |
| | TPR (%) | 90.0 | 65.0 | 90.0 | 55.0 | 55.0 | 85.0 |
| | TNR (%) | 58.3 | 91.7 | 45.8 | 70.8 | 95.8 | 91.7 |
| F0-2 vs F3-4 (≥ F3) | AUC (95%CI) | 0.920 (0.798-0.980) | 0.807 (0.660-0.910) | 0.624 (0.465-0.765) | 0.663 (0.504-0.798) | 0.705 (0.549-0.883) | 0.978 (0.881-0.999) |
| | <i>P</i> | < 0.0001 | 0.0002 | 0.21 | 0.107 | 0.0392 | < 0.0001 |
| | YI | 0.818 | 0.546 | 0.273 | 0.363 | 0.485 | 0.939 |
| | Cutoff | > 11.033 | > 8.385 | ≤ 0.938 | ≤ 0.0330 | ≤ 0.587 | > 0.124 |
| | TPR (%) | 90.9 | 72.7 | 54.6 | 63.6 | 54.6 | 100.0 |
| | TNR (%) | 90.9 | 81.8 | 72.7 | 72.7 | 93.9 | 93.9 |
| F0-3 vs F4 (F4) | AUC (95%CI) | 0.855 (0.716-0.943) | 0.925 (0.805-0.983) | 0.638 (0.480- 0.777) | 0.796 (0.648-0.902) | 0.798 (0.650-0.904) | 0.947 (0.835-0.992) |
| | <i>P</i> | < 0.0001 | < 0.0001 | 0.272 | 0.0058 | 0.0058 | < 0.0001 |
| | YI | 0.702 | 0.790 | 0.377 | 0.597 | 0.561 | 0.807 |
| | Cutoff | > 13.000 | > 8.385 | ≤ 0.938 | ≤ 0.030 | ≤ 0.587 | > 0.383 |
| | TPR (%) | 83.3 | 100.0 | 66.7 | 83.3 | 66.7 | 83.3 |
| | TNR (%) | 86.8 | 79.0 | 71.1 | 76.3 | 89.5 | 97.4 |

¹There is statistically significance when compared with two dimensional shear wave elastography group (*P* < 0.05).

PRE: Predictive value of combined diagnosis; AUC: The area under the ROC curve; YI: Youden index; Cutoff: The diagnostic cut-off point; TPR: The true positive rate; TNR: The true negative rate.

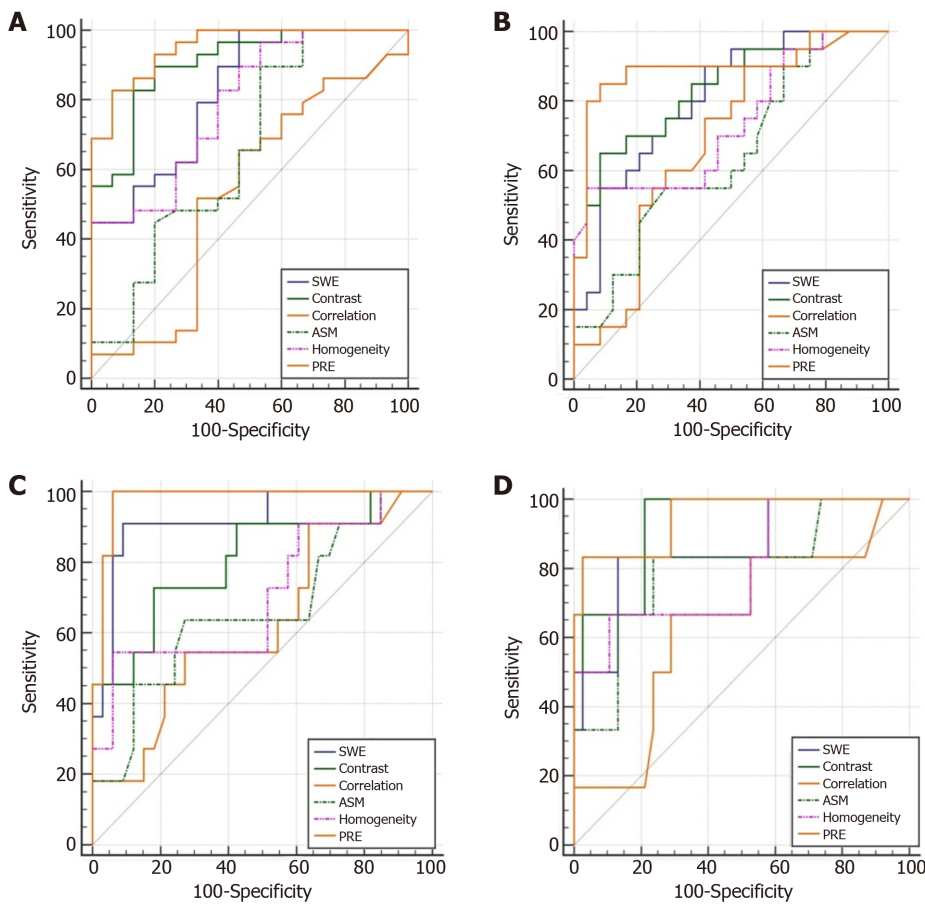


Figure 2 Receiver operating characteristic curves. A: F0 vs F1-4 ($\geq F1$); B: F0-1 vs F2-4 ($\geq F2$); C: F0-2 vs F3-4 ($\geq F3$); D: F0-3 vs F4 (F4). SWE: Shear wave elastography; ASM: Angular second moment; PRE: Predictive value.

ARTICLE HIGHLIGHTS

Research background

Two dimensional shear wave elastography (2D-SWE) has been widely used in non-invasive diagnosis of liver fibrosis due to its non-invasiveness, reproducibility and high accuracy. However, it is not effective in the diagnosis of early liver fibrosis and it is not completely replaceable with liver biopsy; therefore, how to further improve the diagnostic efficacy of 2D-SWE examination on liver fibrosis staging is a clinically urgent problem. Texture analysis has always been a hotspot of image analysis, and texture analysis of medical images has also been achieved good results in the diagnosis and treatment of many diseases. But there are few studies on texture analysis for ultrasound elastic images currently. The combination of the two is expected to improve the diagnostic efficacy of liver fibrosis, especially early liver fibrosis in patients with chronic hepatitis B.

Research motivation

In order to improve the efficacy of non-invasive diagnosis of early liver fibrosis in patients with chronic hepatitis B, the information of elastic images obtained by 2D-SWE examination should be fully applied. This study intends to use the texture analysis software to deeply analyze the elastic images and obtain the spatial distribution information of elastic modulus, meanwhile, combined with the Young's modulus value to diagnose the liver fibrosis. It will provide a new idea and method for the diagnosis of liver fibrosis in patients with chronic hepatitis B.

Research objectives

The objective of this study was to find a non-invasive, reproducible, and accurate method for the diagnosis of early liver fibrosis caused by chronic hepatitis B. The study demonstrated that combination of 2D-SWE with texture analysis can effectively improve the diagnostic efficacy of early liver fibrosis, which provides theoretical support for the application of texture analysis in the diagnosis of early liver fibrosis in patients with chronic hepatitis B, and it also provides a possibility for non-invasive diagnosis to gradually replace the liver tissue biopsy.

Research methods

Based on the 2D-SWE examination, this study applied texture analysis software (SSI) to obtain the mean values at different angles of four texture patterns (contrast, correlation, ASM and

homogeneity). Take pathological results of biopsy specimens as the gold standards to orderly test: comparison and assessment of the diagnosis efficiency conducted for 2D-SWE, contrast, correlation, ASM, homogeneity and their combination. The feasibility of 2D-SWE combined texture analysis in the diagnosis of liver fibrosis was discussed by analyzing the spatial distribution characteristics of elastic modulus, and combined with the application of Young's modulus value.

Research results

The study demonstrated that contrast and homogeneity have separated diagnostic efficacy in the diagnosis of liver fibrosis in patients with chronic hepatitis B. The AUC values of each group in the combined diagnosis are improved compared with the separated diagnosis of each index. The combined diagnosis showed higher diagnosis efficiency over 2D-SWE in early liver fibrosis. This study is the first to apply the texture analysis of elastic images to the non-invasive diagnosis of liver fibrosis, and confirmed the value of contrast and homogeneity in the diagnosis of liver fibrosis, and found that combined diagnosis can improve the diagnostic efficacy of early liver fibrosis. In the further study, it is necessary to continue to explore the influence of different angles on the diagnostic performance of texture features and the feasibility of combined application with other liver fibrosis diagnostic prediction models.

Research conclusions

The main conclusions of this study are as follows: (1) Texture analysis of elastic images can be applied in the diagnosis of liver fibrosis with chronic hepatitis B, in which the diagnostic efficacy of contrast and homogeneity is comparable to 2D-SWE, but correlation and ASM showed poor diagnosis efficiency; (2) Combined diagnosis (2D-SWE plus texture analysis) can effectively improve the diagnostic efficacy of liver fibrosis in patients with chronic hepatitis B, especially in the diagnosis of early liver fibrosis, combined diagnostic efficacy is better; and (3) The staging of liver fibrosis in chronic hepatitis B may be related to the spatial heterogeneity of liver tissue hardness distribution. The more spatial heterogeneity of hardness distribution, the more severe the degree of liver fibrosis.

Research perspectives

This study confirmed that the post-processing of elastic images can further improve the diagnostic value of ultrasound-elastic images for liver fibrosis. However, the sample size of this study is small, and other diagnostic indicators related to liver fibrosis have not been combined. A robust diagnosis model of liver fibrosis has not yet been established. In the follow-up study, while optimizing the texture analysis, the sample size will be expanded, and other liver fibrosis diagnostic methods may be combined to establish a non-invasive diagnostic model for early liver fibrosis with higher efficacy.

REFERENCES

- 1 **Lefton HB**, Rosa A, Cohen M. Diagnosis and epidemiology of cirrhosis. *Med Clin North Am* 2009; **93**: 787-799, vii [PMID: 19577114 DOI: 10.1016/j.mcna.2009.03.002]
- 2 **Bedossa P**, Dargère D, Paradis V. Sampling variability of liver fibrosis in chronic hepatitis C. *Hepatology* 2003; **38**: 1449-1457 [PMID: 14647056 DOI: 10.1016/j.hep.2003.09.022]
- 3 **Kose S**, Ersan G, Tatar B, Adar P, Sengel BE. Evaluation of Percutaneous Liver Biopsy Complications in Patients with Chronic Viral Hepatitis. *Eurasian J Med* 2015; **47**: 161-164 [PMID: 26644763 DOI: 10.5152/eurasianjmed.2015.107]
- 4 **Bamber J**, Cosgrove D, Dietrich CF, Fromageau J, Bojunga J, Calliada F, Cantisani V, Correas JM, D'Onofrio M, Drakonaki EE, Fink M, Friedrich-Rust M, Gilja OH, Havre RF, Jenssen C, Klausner AS, Ohlinger R, Saftoiu A, Schaefer F, Sporea I, Piscaglia F. EFSUMB guidelines and recommendations on the clinical use of ultrasound elastography. Part 1: Basic principles and technology. *Ultraschall Med* 2013; **34**: 169-184 [PMID: 23558397 DOI: 10.1055/s-0033-1335205]
- 5 **Dietrich CF**, Bamber J, Berzigotti A, Bota S, Cantisani V, Castera L, Cosgrove D, Ferraioli G, Friedrich-Rust M, Gilja OH, Goertz RS, Karlas T, de Knegt R, de Ledinghen V, Piscaglia F, Procopet B, Saftoiu A, Sidhu PS, Sporea I, Thiele M. EFSUMB Guidelines and Recommendations on the Clinical Use of Liver Ultrasound Elastography, Update 2017 (Long Version). *Ultraschall Med* 2017; **38**: e16-e47 [PMID: 28407655 DOI: 10.1055/s-0043-103952]
- 6 **Ferraioli G**, Filice C, Castera L, Choi BI, Sporea I, Wilson SR, Cosgrove D, Dietrich CF, Amy D, Bamber JC, Barr R, Chou YH, Ding H, Farrok A, Friedrich-Rust M, Hall TJ, Nakashima K, Nightingale KR, Palmeri ML, Schafer F, Shiina T, Suzuki S, Kudo M. WFUMB guidelines and recommendations for clinical use of ultrasound elastography: Part 3: liver. *Ultrasound Med Biol* 2015; **41**: 1161-1179 [PMID: 25800942 DOI: 10.1016/j.ultrasmedbio.2015.03.007]
- 7 **Li Y**, Huang YS, Wang ZZ, Yang ZR, Sun F, Zhan SY, Liu XE, Zhuang H. Systematic review with meta-analysis: the diagnostic accuracy of transient elastography for the staging of liver fibrosis in patients with chronic hepatitis B. *Aliment Pharmacol Ther* 2016; **43**: 458-469 [PMID: 26669632 DOI: 10.1111/apt.13488]
- 8 **Feng JC**, Li J, Wu XW, Peng XY. Diagnostic Accuracy of SuperSonic Shear Imaging for Staging of Liver Fibrosis: A Meta-analysis. *J Ultrasound Med* 2016; **35**: 329-339 [PMID: 26795041 DOI: 10.7863/ultra.15.03032]
- 9 **Leung VY**, Shen J, Wong VW, Abrigo J, Wong GL, Chim AM, Chu SH, Chan AW, Choi PC, Ahuja AT, Chan HL, Chu WC. Quantitative elastography of liver fibrosis and spleen stiffness in chronic hepatitis B carriers: comparison of shear-wave elastography and transient elastography with liver biopsy correlation. *Radiology* 2013; **269**: 910-918 [PMID: 23912619 DOI: 10.1148/radiol.13130128]
- 10 **Jiang H**, Zheng T, Duan T, Chen J, Song B. Non-invasive in vivo Imaging Grading of Liver Fibrosis. *J Clin Transl Hepatol* 2018; **6**: 198-207 [PMID: 29951365 DOI: 10.14218/JCTH.2017.00038]

- 11 **Caviglia GP**, Abate ML, Pellicano R, Smedile A. Chronic hepatitis B therapy: available drugs and treatment guidelines. *Minerva Gastroenterol Dietol* 2015; **61**: 61-70 [PMID: 25323305]
- 12 **Vallet-Pichard A**, Pol S. Hepatitis B virus treatment beyond the guidelines: special populations and consideration of treatment withdrawal. *Therap Adv Gastroenterol* 2014; **7**: 148-155 [PMID: 25057295 DOI: 10.1177/1756283X14524614]
- 13 **Jeong JY**, Kim TY, Sohn JH, Kim Y, Jeong WK, Oh YH, Yoo KS. Real time shear wave elastography in chronic liver diseases: accuracy for predicting liver fibrosis, in comparison with serum markers. *World J Gastroenterol* 2014; **20**: 13920-13929 [PMID: 25320528 DOI: 10.3748/wjg.v20.i38.13920]
- 14 **Chon YE**, Choi EH, Song KJ, Park JY, Kim DY, Han KH, Chon CY, Ahn SH, Kim SU. Performance of transient elastography for the staging of liver fibrosis in patients with chronic hepatitis B: a meta-analysis. *PLoS One* 2012; **7**: e44930 [PMID: 23049764 DOI: 10.1371/journal.pone.0044930]
- 15 **Dong DR**, Hao MN, Li C, Peng Z, Liu X, Wang GP, Ma AL. Acoustic radiation force impulse elastography, FibroScan®, Forns' index and their combination in the assessment of liver fibrosis in patients with chronic hepatitis B, and the impact of inflammatory activity and steatosis on these diagnostic methods. *Mol Med Rep* 2015; **11**: 4174-4182 [PMID: 25651500 DOI: 10.3892/mmr.2015.3299]
- 16 **Kanamoto M**, Shimada M, Ikegami T, Uchiyama H, Imura S, Morine Y, Kanemura H, Arakawa Y, Nii A. Real time elastography for noninvasive diagnosis of liver fibrosis. *J Hepatobiliary Pancreat Surg* 2009; **16**: 463-467 [PMID: 19322509 DOI: 10.1007/s00534-009-0075-9]
- 17 **Cassinotto C**, Lapuyade B, Mouries A, Hiriart JB, Vergniol J, Gaye D, Castain C, Le Bail B, Chermak F, Foucher J, Laurent F, Montaudon M, De Ledinghen V. Non-invasive assessment of liver fibrosis with impulse elastography: comparison of Supersonic Shear Imaging with ARFI and FibroScan®. *J Hepatol* 2014; **61**: 550-557 [PMID: 24815876 DOI: 10.1016/j.jhep.2014.04.044]
- 18 **Guibal A**, Renosi G, Rode A, Scoazec JY, Guillaud O, Chardon L, Munteanu M, Dumortier J, Collin F, Lefort T. Shear wave elastography: An accurate technique to stage liver fibrosis in chronic liver diseases. *Diagn Interv Imaging* 2016; **97**: 91-99 [PMID: 26655870 DOI: 10.1016/j.diii.2015.11.001]
- 19 **Zeng J**, Liu GJ, Huang ZP, Zheng J, Wu T, Zheng RQ, Lu MD. Diagnostic accuracy of two-dimensional shear wave elastography for the non-invasive staging of hepatic fibrosis in chronic hepatitis B: a cohort study with internal validation. *Eur Radiol* 2014; **24**: 2572-2581 [PMID: 25027837 DOI: 10.1007/s00330-014-3292-9]
- 20 **Mancini M**, Salomone Megna A, Ragucci M, De Luca M, Marino Marsilia G, Nardone G, Coccoli P, Prinster A, Mannelli L, Vergara E, Monti S, Liuzzi R, Incoronato M. Reproducibility of shear wave elastography (SWE) in patients with chronic liver disease. *PLoS One* 2017; **12**: e0185391 [PMID: 29023554 DOI: 10.1371/journal.pone.0185391]
- 21 **Huang C**, Pan X, He Q, Huang M, Huang L, Zhao X, Yuan C, Bai J, Luo J. Ultrasound-Based Carotid Elastography for Detection of Vulnerable Atherosclerotic Plaques Validated by Magnetic Resonance Imaging. *Ultrasound Med Biol* 2016; **42**: 365-377 [PMID: 26553205 DOI: 10.1016/j.ultrasmedbio.2015.09.023]
- 22 **Bhatia KS**, Lam AC, Pang SW, Wang D, Ahuja AT. Feasibility Study of Texture Analysis Using Ultrasound Shear Wave Elastography to Predict Malignancy in Thyroid Nodules. *Ultrasound Med Biol* 2016; **42**: 1671-1680 [PMID: 27126245 DOI: 10.1016/j.ultrasmedbio.2016.01.013]
- 23 **Haralick R**, Shanmuga K, Dinstein I. Textural Features for Image Classification. *IEEE Trans Syst Man Cybern* 1973; **3**: 610-621
- 24 **Valckx FM**, Thijssen JM. Characterization of echographic image texture by cooccurrence matrix parameters. *Ultrasound Med Biol* 1997; **23**: 559-571 [PMID: 9232765]
- 25 **Huang C**, He Q, Huang M, Huang L, Zhao X, Yuan C, Luo J. Non-Invasive Identification of Vulnerable Atherosclerotic Plaques Using Texture Analysis in Ultrasound Carotid Elastography: An In Vivo Feasibility Study Validated by Magnetic Resonance Imaging. *Ultrasound Med Biol* 2017; **43**: 817-830 [PMID: 28153351 DOI: 10.1016/j.ultrasmedbio.2016.12.003]



Published By Baishideng Publishing Group Inc
7041 Koll Center Parkway, Suite 160, Pleasanton, CA 94566, USA
Telephone: +1-925-2238242
Fax: +1-925-2238243
E-mail: bpgoffice@wjgnet.com
Help Desk: <https://www.f6publishing.com/helpdesk>
<https://www.wjgnet.com>

